Research Article

Assessment Of Cl 2 /CHF 3 Mixture For Plasma Etching Process On Barc And Tin Layer For 0.21 µm Metal Line: Silterra Case Study

Wan Faizal Mohamed-Hassan[1], Kader Ibrahim[2], Mohd Azizi Chik[3], Ghazali Omar[4], Noreffendy Bin Tamaldin[5]

[1]Etch, SlTerra Malaysia Sdn. Bhd., Kedah, Malaysia,
[2]Fab Operation, SilTerra Malaysia Sdn. Bhd., Kedah, Malaysia,
[3]Integrated Module, SilTerra Malaysia Sdn. Bhd, Kedah, Malaysia
[4]Faculty of Mechanical, University of Technical Melaka, Melaka, Malaysia,
[5]Faculty of Mechanical, University of Technical Melaka, Melaka, Malaysia,

Article History : Received :11 January 2021; Accepted: 27 February 2021; Published online: 5 April 2021

ABSTRACT :In wafer fabrication manufacturing, aluminum etching process is a dry plasma etching process used as main process for construction of aluminum (Al) interconnects structures. As customer requirement changed for faster, more reliable and lower cost chips, chip manufacturers have learned to reduce the size of component on a chip in order to achieve those requirements(Ibrahim, Chik, & Hashim, 2016). As the geometry of the chip getting smaller, the width of Al line wiring specification also shrinking. To print the smaller geometry pattern requirement, the thickness in masking process also has to be reduced for better resolution. Such a thinner resist will create a challenge during plasma etching to ensure a minimal resist loss process which required new type of equipment but this research insist to sustain similar equipment. The use of oxide film as a hard mask has been evaluated by other researchers but alternative approach still needed to suit specific requirement of semiconductor factory installation base. This approach does require a process integration change and require a full technology qualification and easily take a lengthy qualification procedures especially when to qualify the existing products. It is worth trying at the situation of no other solution available. The challenge of insufficient margin for the metal line etching process for 0.2 µm width has caused the deformed metal pattern formation. This chemistry study of Cl_2/CHF_3 as a replacement gas to existing Cl_2/O_2 to address Organic backside anti refractive coating (OBARC) was evaluated and proven novelty where detail discussed in the following content.

KEYWORDS: Aluminum, plasma etching, Cl2/CHF3, BARC, TiN

INTRODUCTION

The patterning of aluminum metal interconnect structures is complicated by the multilayer of metallization scheme adopted by industry for IC production. In advanced metallization scheme (Pramanik & Saxena, 1983; Wilson, Tracy, & Freeman, 1993), the aluminum film which is often alloyed with copper serves as the conductor and is sandwiched by the barrier layers of titanium nitride (TiN) layer on the top and by TiN and titanium (Ti) layers at the bottom (Filippi et al., 2001). The purpose of this barrier layers are to avoid the inter-diffusion of aluminum and silicon ("Spiking"). The spiking occurs when the silicon becomes soluble into aluminum film as the temperature increases. The main reason for the complexity is to enhance the electromigration resistance in the device (Hosaka, Kouno, Hayakawa, Niwa, & Yamada, 1998; M. H. Lee et al., 2011). Etching of these films require multi step etching process with different mixture of chemistry (Vignes & Baléo, 1997) combined with optimum power (Kim, Jung, Choi, Kim, & Boo, 2005) and pressure conditions (Christie, 1994; Kunz, 2007; Okumura, 2010) to ensure the metal etching profile meeting the process requirements. The very fundamental requirement in plasma etching method adopted in fabricating of an IC pattern is the photoresist remaining margin. The pre-defined photoresist pattern on the metal substrate during photolithography process comes together with the organic backside anti-refractive coating film to improve reflection control and light absorption during photolithography(Boumerzoug, 2014; Huang & Weigand, 2008; Zhuang et al., 2006). BARC layer minimizes thin film interference effects by reducing reflected light.

In the patterning transfer, during BARC opening process, high etch selectivity of resist to BARC process is required to minimize the resist loss to allow further substrate etching (Armacost et al., 1999). BARC also must etch quickly to prevent line width change. The selectivity of BARC to resist depend mainly on the carbon content and also its composition and structure responses towards oxidizing gas, reducing gas and plasma bombardment. As the geometry of the chip getting smaller, the width of Al line wiring specification also shrinking. To print the smaller geometry pattern requirement, the thickness in masking process also has to be reduced for better resolution. Such a thinner resist will create an inconsistency of the pattern width and unable to produce straight profile requirement if

having insufficient of resist remaining process during plasma etching (H. J. Lee et al., 2008). This failure will lead to device electrical. Therefore, an optimized matching metal etching process is required. Further assessment in the following content will discuss finding of Cl_2/CHF_3 mixture to etch BARC and top TiN layer of metallization film having minimum metal line geometry of 0.21µm line and space.

METHODS

Figure 1 explainsworkflow of the methodology adopted in this assessment of Cl_2/CHF_3 in BARC and TiN Etching of AlCumetallization interconnect.

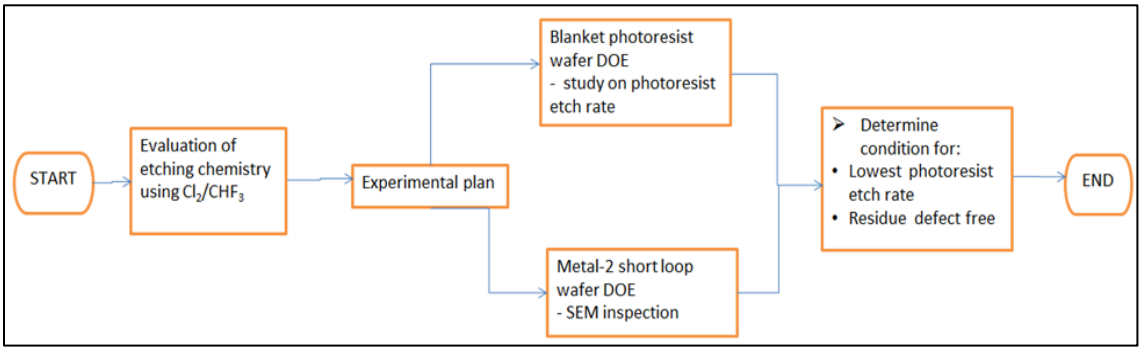

Figure 1: Methodology approach

The assessment was divided into two parts. The first part of the evaluation was done on the blanket photoresist wafers to determine the photoresist etch rate at different combinations of Cl_2 and CHF_3 flow rates combinations as tabulated in Table 1. The evaluation was done on the blanket photoresist wafers coated on bare silicon wafers with thickness of 14000Å. A ThermawaveOptiprobe metrology tool was used to measure the film thickness of photoresist before and after the plasma etching process. Each wafer was etched in inductively coupled plasma (ICP) metal etcher system at the cathode temperature of 40C. The remaining process parameters and equipment parameters were remained as constant. The photoresist etch rate were determined for each of the conditions and analyzed.

Slot	Pattern	Cl_2 Flow (sccm)	CHF_3 Flow (sccm)
1	++	75	20
2	+-	75	10
3	-+	25	20
4	--	25	10
5	00	50	15
6	00	50	15
7	+-	60	0

Table 1: Experimental conditions of Cl_2 and CHF_3 flow rates combinations for photoresist etch rate study

In the second part of the assessment, the evaluation was done in the same metal etcher tool using pattern wafer instead of blanket photoresist wafers. The metal film of 0.40 µm stack (TiN/AlCu/TiN/Ti) was deposited after the dieletric layer formation on bare Si wafer. AlCu alloy where the Cu concentration is 0.5 wt.% and the AlCu is deposited at 350℃. The wafers were patterned with 7750Å DUV photoresist on 700Å of organic BARC film. The reticle mask used in this experiment from the customer reticle of metal-2 layer having 0.2 µm minimum design rules of line and space. Total of 8 wafers were prepare. The samples ware etched in ICP metal etcher tool using multiple etching step method as summarized in Table 2 below. The metal-2 etching recipes consist of six (6) etching steps.

Step	Etch process description
1	PR hardening
2	BARC etching

3	TiN etching
4	BT etching
5	ME EPD etching
6	OE (IMD Recess)

Table 2: Metal-2 multiple etching step recipe with process steps descriptions

The evaluation of Cl_2/CHF_3 mixture combinations were applied in BARC etching (Step2) and TiN etching (Step3) using similar gas ratio as tabulated in Table 3.The table was designed based on full factorial DOE to characterize the etching characteristic on the residue defects in open etching area. The rest of the etching step conditions were remained as constant.

Run	Pattern	Factor 1 Cl_2	Factor 2 CHF_3
1	--	40	12
2	00	50	15
3	-+	40	18
4	+-	60	12
5	++	60	18
6	+-	45	12
7	++	45	18
8	++	55	15

Table 3: Cl_2/CHF_3 flow rate combinations applied on Step 2 and Step 3 of Metal-2 etching recipe

All the completed etching wafers were processed in solvent cleaning tool for polymer removal steps. The SEM inspection was done on all samples at center die and edge die of the wafers. The inspection point covered the isolated and dense metal line structures with 2µm field of view (FOV) SEM image captured. The observed residue defects in each SEM images were counted and tabulated for further statistical analysis

RESULTS AND DISCUSSION

The result of photoresist etch rate obtained from the experimental run was tabulated in Table 4 below. The sample mean etch rate for each run is tabulated and its respective confidence interval (CI) is determined at 95% confidence level. The statistical analysis is done based on the upper CI value.

Slot	Pattern	Cl2 Flow rate (sccm)	CHF3 Flow rate (sccm)	Sample Mean (Å/min)	Lower CI (Å/min)	Upper CI (Å/min)
1	++	75	20	1216	1191	1241
2	+-	75	10	1150	1124	1177
3	-+	25	20	896	867	925
4	--	25	10	858	831	886
5	00	50	15	1101	1077	1126
6	00	50	15	1032	1011	1053
7	+-	60	0	1050	1020	1080

Table 4: Sample mean of photoresist etch rate for each run

Figure 2 shows the Y-axis of PRERactual value from upper CI and X-axis is the PRER Predicted value obtained by the proposed model derived from the fit model analysis. The suggested model of predicted PRER obtained in this experiment analysis is statistically significant as the RSq is 0.96 and the Pvalue is 0.0152 as tabulated in Table 5 and Table 6 respectively.

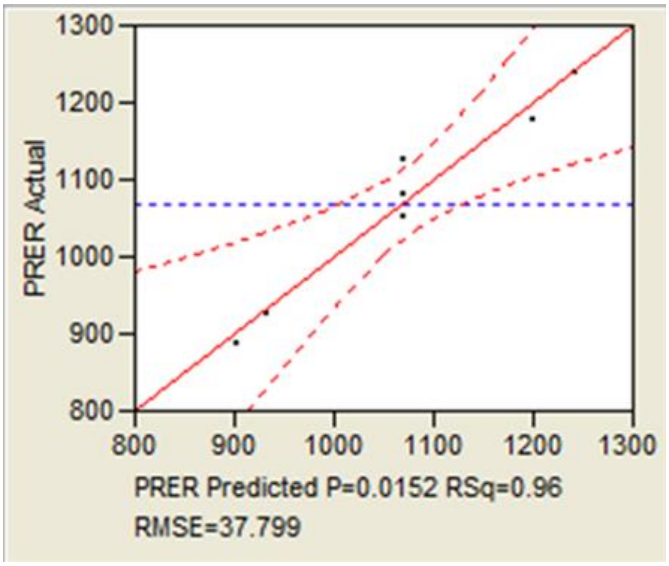

Figure 2: Correlation of PRER Actual against PRER Predicted with RSq=0.96 and Pvalue of 0.0152 suggesting a significant experimental model.

RSquare	0.96
RSquareAdj	0.91
Root Mean Square Error	37.80
Mean of Response	1069.43
Observations (or Sum Wgts)	7

Table 5: Summary of Fit

Source	DF	Sum of Squares	Mean Square	F Ratio
Model	3	94355.423	31451.8	22.0133
Error	3	4286.291	1428.8	Prob> F
C. Total	6	98641.714		0.0152

Table 6: Analysis of Variance

From the parameter estimate in Table 7, photoresist etch rate (PRER) using Cl_2/CHF_3 plasma significantly dependent on the Cl_2 flow. The CHF_3 flow is not significant and no interaction exist in this model as the Pvalue for both terms (CHF_3 and Cl2*CHF3) are greater than 0.05.

Term	Estimate	Std Error	t Ratio	Prob>|t|
Intercept	1069.214	15.09068	70.85	<.0001
Cl2(25,75)	152.42838	18.8002	8.11	0.0039
CHF3(10,20)	18.537118	12.10867	1.53	0.2233
Cl2*CHF3	3.2148472	17.98609	0.18	0.8695

Table 7: Parameter estimates of each term with P-value <0.05 indicates its significant in the model.

Figure 4(a) and (b) shows the leverage plots for the Cl_2 and CHF_3 effect respectively. The Y-axis is the predicated response of photoresist etch rate when the magnitude of factor in X-axis is varied. The leverage plot for Cl_2 having steeper slope than for CHF_3 suggesting that CHF_3 factor does effect PRER however it is less significant as compared to Cl_2 factor. Therefore the use of CHF_3 in BARC etching step is able to preserve the photoresist margin. This is an advantage to process engineer as the factor may be considered as the nob to control the lateral etching of the metal width dimension (FICD) without significantly degrade the photoresist margin. Moreover, CHF_3 is one of the polymerizing chemistry that generates polymeric material on wafer surface when used in RF plasma condition (Astell-Burt et al., 1986). Saito et. al reported in his study that CHF_3 used in etching aluminum film able to control the metal width dimension by suppressing side wall etching of the aluminum due to the passivation layer deposited on the sidewall of the resist and aluminum pattern. In this application, we propose to use the CHF_3 gas in BARC etching to generate polymer film and deposited on the sidewall of the photo resist pattern with the expectation to minimize lateral etching to the resist and able to minimize the width dimension shift of the mask pattern. Based on this qualitative study, the use of CHF_3 in the BARC step will reduce the shift in photo resist width dimension during BARC opening step and able to control CD as required. The flow margin of CHF_3 has to be determined to ensure the BARC film is not overly polymerized by the carbon based species and no micromasking defect in the underneath TiN ARC film is formed. Failure to clear the BARC film in the open area and the creation of micromasking defect during TiN etching step will lead to post metal etch residue defect in the opening area (Lee et al., 2008).

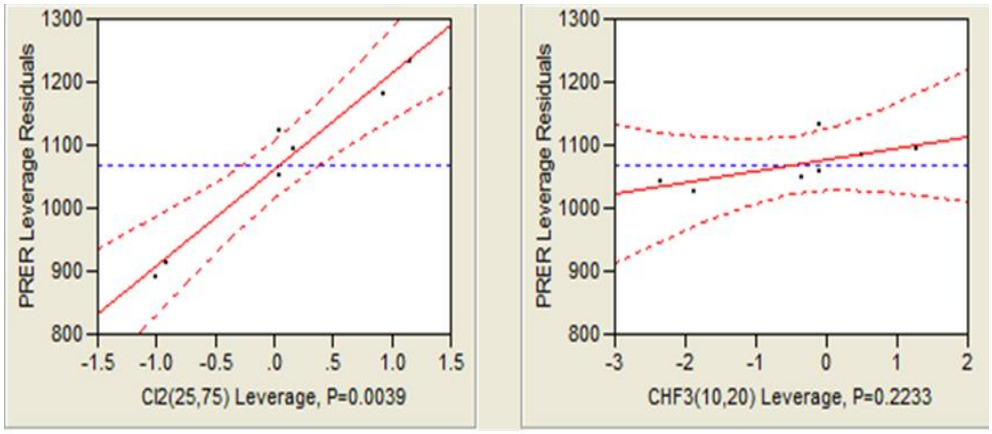

(a) (b)

Figure 3: The Leverage Plot for (a) Cl_2 and (b) CHF_3 factor

Table 5 shows the result of the second part of experiment evaluated on patterned wafers using Metal-2 reticle mask. Total defect counts was counted based on the SEM micrograph image captured at center die and edge die of each sample as shown by Figure 5 and 6 below. Total of 65 counts of defects were recorded for the Run#7 SEM micrograph images inspected at isolated (MPISO) and dense (MPDense) region structures on both die locations.

Run	Pattern	Factor 1 (Cl2)	Factor 2 (CHF3)	Total defect counts
1	--	40	12	4
2	00	50	15	0
3	-+	40	18	79
4	+-	60	12	0
5	++	60	18	4
6	+-	45	12	0
7	++	45	18	65
8	++	55	15	0

Table 8: Results of defect residues

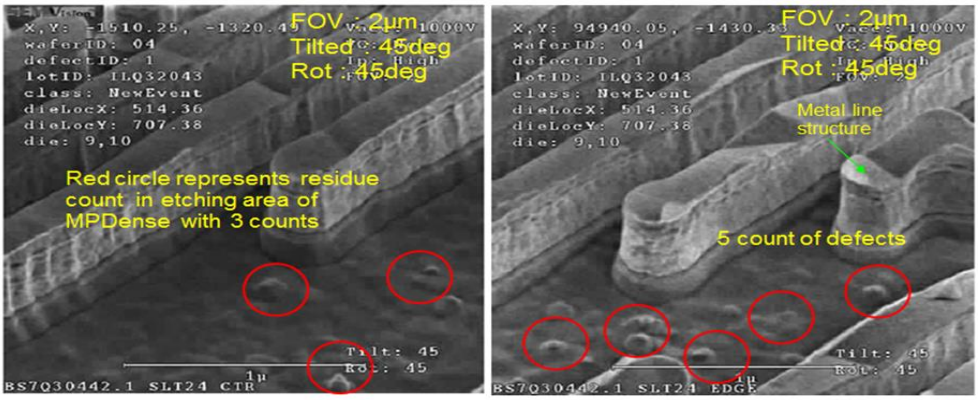

(a) (b)

Figure 4: SEM Images for Run 7 at MPDense (a) center, (b) edge

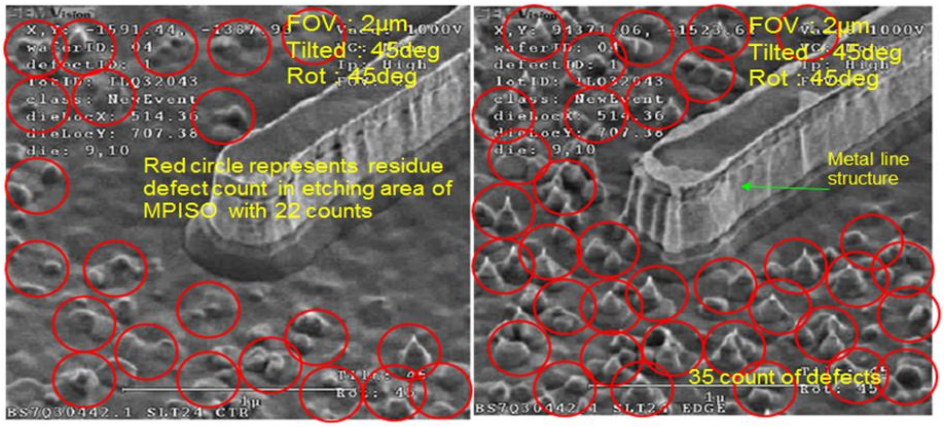

(a) (b)

Figure 5: SEM Images for Run7 at MPISO (a) center, (b) edge

Figure 7 suggests experimental model on residue defects counts response shows the R-Square value greater than 0.9 and the p-value of the ANOVA is statistically significant, 0.0076. Table 9 shows all the 3 experimental terms (Cl_2, CHF_3 and Cl_2*CHF_3) analyzed in this model found to be significant on the residue defect count response with p-value of less than 0.05.

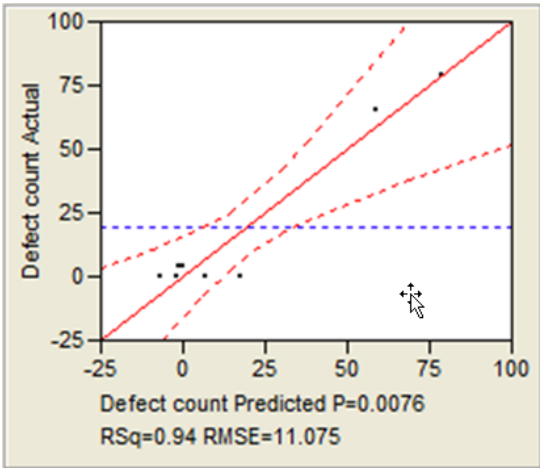

Figure 6: Correlation of Residue defect count Actual against Predicted value with RSq=0.94 and Pvalue of 0.0076 suggesting a significant experimental model

Term	Estimate	Std Error	t Ratio	Prob>|t|
Intercept	17.649007	3.9287	4.49	0.0109
Cl2(40,60)	-21.61589	5.09855	-4.24	0.0133
CHF3(12,18)	20.942308	4.60765	4.55	0.0105
Cl2*CHF3	-18.34615	5.32046	-3.45	0.0261

Table 9: Parameter estimates of each term with P-value <0.05 indicates its significant in the model.

Figure 8 shows the interaction profile between Cl_2 and CHF_3. Based on plot profile, the sensitivity of the CHF_3 flow to the defect residue is minimal when the Cl_2 flow is operating at higher set point. Furthermore, previous work already demonstrated that TiN etch rate is proportional to Cl_2 flow rate (Min et al., 2008). The higher TiN etch rate would reduce the possibility of having TiN residue defects which later may transform into the residue defect at the end of etching process. This condition will maximize the process margin against the residue defect. The adoption of CHF_3 in plasma etching has been reported by previous researcher (H. J. Lee et al., 2008; Saito, Sugita, & Tonotani, 2005) that it would generate polymeric film on the wafer surface that preventing the surface reaction between the main etchant gas and the material to occur. Another researcher reported that the presence of fluorine as an additive with the chlorine as the main etchant would enhance the TiN etch rate performance (Abraham, Gabriel, & Zheng, 1997). However, too high flow of CHF_3 will cause the density of passivation species more than the density of the neutral species. The increase in generation of passivation species may lead to thicker polymerization layer in the etching area and slowing down the reaction of the neutral species with the material to etch. Since the same chemistry mixture was used in BARC and TiN etching steps, we believed the residue defect observed could originate either from BARC or TiN etching step. The unclear BARC or TiN material has transformed into micro-masking defect and locally slow down the etching rate during the subsequent etching steps and remained as residue defect formation.
In this work, we have successfully identified the safe process window of Cl_2 and CHF_3 flow required in metal etching process for BARC and TiN etching steps to ensure zero residue defects.

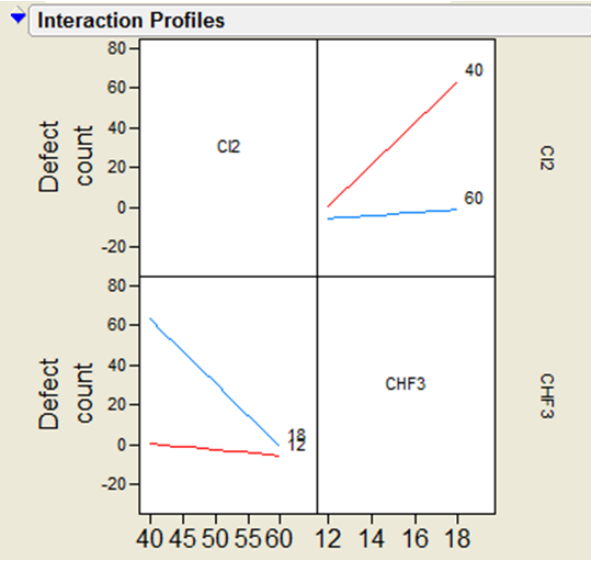

Figure 7: Interaction profile of Cl_2 and CHF_3flowrate on residue defect counts observed in etching area

CONCLUSION

The replacement of Cl_2/O_2chemistry mixture to Cl_2/CHF_3 mixture has enabled us to reduce the photoresistetch rate during the OBARC etchingstep. Our experiment model has suggestedthat CHF_3 flow rate in the mixture has least effect on the photoresistetch rate. The findingis in ageementwithotherresearcher(Kwon, Kim, Lee, Lee, & Park, 2009) investigation that the loweretchrateis due to the formation of CFxpolimerization film.

The samechemistrywasalsoevaluated to etch the TiN ARC layer of the metal-2 film stacks. The characterization on the metalresiduedefectsdonebased on the SEM image micrographanalysisdisclosed the findingthat the low flow of Cl_2wouldinduced the defect formation in the presence of CHF_3species in the mixture. The new alternative solution has been implemented in the real semiconductorprocess application.

ACKNOWLEDGEMENTS

Authors are greatful to SilTerra Malaysia and University of TechnicalMelaka for providingopportunity to carry out thisresearchwork**.**

REFERENCES

1. Abraham, S. C., Gabriel, C. T., & Zheng, J. (1997). Performance of different etch chemistries on titanium nitride antireflective coating layers and related selectivity and microloading improvements for submicron geometries obtained with a high-density metal etcher. *Journal of Vacuum Science & Technology A*, *15*(3), 702–706. https://doi.org/10.1116/1.580805
2. Armacost, M., Hoh, P. D., Wise, R., Yan, W., Brown, J. J., Keller, J. H., … Spuler, B. (1999). Plasma-etching processes for ULSI semiconductor circuits. *IBM Journal of Research and Development*, *43*(1–2), 39–71. https://doi.org/10.1147/rd.431.0039
3. Boumerzoug, M. (2014). Optimized BARC films and etch byproduct removal for wafer edge defectivity reduction. *ASMC (Advanced Semiconductor Manufacturing Conference) Proceedings*, 330–333. https://doi.org/10.1109/ASMC.2014.6847031
4. Christie, R. (1994). Process transfer from conventional RIE to transformer-coupled high density plasma metal etch system. In Anon (Ed.), *IEEE/SEMI Advanced Semiconductor Manufacturing Conference and Workshop* (pp. 34–36).
5. Filippi, R. G., Gribelyuk, M. A., Joseph, T., Kane, T., Sullivan, T. D., Clevenger, L. A., … Rodbell, K. P. (2001). Electromigration in AlCu lines: Comparison of Dual Damascene and metal reactive ion etching. *Thin Solid Films*, *388*(1–2), 303–314. https://doi.org/10.1016/S0040-6090(01)00855-0
6. Hosaka, M., Kouno, T., Hayakawa, Y., Niwa, H., & Yamada, M. (1998). Ti layer thickness dependence on electromigration performance of Ti-AlCu metallization. In *1998 IEEE International Reliability Physics Symposium Proceedings. 36th Annual (Cat. No.98CH36173)* (pp. 329–334). https://doi.org/10.1109/RELPHY.1998.670665
7. Huang, R., & Weigand, M. (2008). Plasma etch properties of organic BARCs. *Advances in Resist Materials and Processing Technology XXV*, *6923*, 69232G. https://doi.org/10.1117/12.772012
8. Ibrahim, K., Chik, M., & Hashim, U. (2016). Semiconductor Fabrication Strategy for Cycle Time and Capacity Optimization : Past and Present. In *Proceedings of the 2016 International Conference on Industrial Engineering and Operations Management* (pp. 2798–2807). IEOM ISBN: 978-0-9855497-4-9.
9. Kim, D. W., Jung, M. Y., Choi, S. S., Kim, J. W., & Boo, J. H. (2005). The effect of SiCl4 additive gas on the Cl-based Al plasma etch procedure. *Thin Solid Films*, *475*(1-2 SPEC. ISS.), 81–85. https://doi.org/10.1016/j.tsf.2004.07.042
10. Kunz, R. R. (2007). *Dry etching of photoresists*. *Microlithography: Science and Technology, Second Edition*.
11. Kwon, B. S., Kim, J. S., Lee, N. E., Lee, S. K., & Park, S. W. (2009). Comparative study on the etching characteristics of ArF and EUV resists in dual-frequency superimposed capacitively-coupled CF 4/O 2/Ar and CF 4/CHF 3/O 2/Ar plasmas. *Journal of the Korean Physical Society*, *55*(4), 1465–1471. https://doi.org/10.3938/jkps.55.1465
12. Lee, H. J., Hung, C. L., Leng, C. H., Lian, N. T., Young, L. W., Yang, T., … Lu, C. Y. (2008). Etch defect characterization and reduction in hard-mask-based Al interconnect etching. *International Journal of Plasma Science and Engineering*, *2008*. https://doi.org/10.1155/2008/154035
13. Lee, M. H., Kwon, Y. M., Pyo, S. G., Lee, H. C., Han, J. W., & Paik, K. W. (2011). Effects of metal stacks and patterned metal profiles on the electromigration characteristics in super-thin AlCu interconnects for sub-0.13 µm technology. *Thin Solid Films*, *519*(11), 3906–3913. https://doi.org/10.1016/j.tsf.2011.01.268
14. Min, S. R., Cho, H. N., Li, Y. L., Lim, S. K., Choi, S. P., & Chung, C. W. (2008). Inductively coupled plasma reactive ion etching of titanium nitride thin films in a Cl2/Ar plasma. *Journal of Industrial and Engineering Chemistry*, *14*(3), 297–302. https://doi.org/https://doi.org/10.1016/j.jiec.2008.01.001
15. Okumura, T. (2010). Inductively coupled plasma sources and applications. *Physics Research International*, *2010*(1). https://doi.org/10.1155/2010/164249
16. Pramanik, D., & Saxena, A. N. (1983). VLSI METALLIZATION USING ALUMINUM AND ITS ALLOYS - 1. *Solid State Technology*, *26*(1), 127–133.

17. Saito, S., Sugita, K., & Tonotani, J. (2005). Effect of CHF 3 Addition on Reactive Ion Etching of Aluminum Using Inductively Coupled Plasma. *Japanese Journal of Applied Physics*, *44*(5A), 2971–2975. https://doi.org/http://dx.doi.org/10.1143/JJAP.44.2971
18. Vignes, M. J., & Baléo, J. N. (1997). Experimental investigation of a Cl2/BCl3/N2 chemistry based aluminium plasma etching. *Vide: Science, Technique et Applications*, *53*(284 SUPPL. 1), 41–43.
19. Wilson, S. R., Tracy, C. J., & Freeman, J. L. (1993). *Handbook of Multilevel Metallization for Integrated Circuits: Materials, Technology and Applications (Materials Science and Process Technology)*. New Jersey: Noyes Publications.
20. Zhuang, H., Abdallah, D., Xiang, Z., Wu, H., Shan, J., Lu, P.-H., … Badowski, P. R. (2006). The effects of etch chemistry on the etch rates of ArF BARC products. *Advances in Resist Technology and Processing XXIII*, *6153*, 61530N. https://doi.org/10.1117/12.657128